A statistical model to predict bone cell diffusion patterns in scaffolds

*Wilson Fok¹, S.T.C. Lin³, D. Musson², J. Cornish², †J.W. Fernandez^{1,4}

¹ Auckland Bioengineering Institute, the University of Auckland, Auckland 1010, New Zealand.
² Department of Medicine, the University of Auckland, Auckland, New Zealand.

*Presenting author: wfok007@aucklanduni.ac.nz †Corresponding author: j.fernandez@auckland.ac.nz

Extended Abstract

Keywords: mass diffusion, finite element method, transductive learning, support vector regression

Introduction

This study is motivated by the challenges in estimating bone cell diffusivity for a scaffold. Bone cell diffusion is based on numerous factors including the scaffold architecture, cell differentiation and clustering within the scaffold pores and temporal factors over time. While we can observe cell staining on histology slides to estimate the degree of cell proliferation, this is typically only for a 2D slice and does not represent the entire scaffold. Alternatively, 3D computational models of cell differentiation provide a tool to predict cell diffusion given geometry, initial cell concentration and diffusion values. However, the biology is far more complicated than a simple continuum diffusion analysis can reveal. In this study we propose a different computational approach whereby a statistical model is developed using machine learning. In this way the more biological information available the better the model can predict the diffusion. The idea is to develop 100's of synthetic models of diffusion that are used to link diffusion with cell concentration patterns. We can then reverse engineer this by obtaining real temporal cell concentration patterns in scaffolds to reveal the likely scaffold diffusion. This study presents our preliminary results.

Methods

Experimental: The experimental scaffold data for this study came from a previous PhD thesis. Specifically, PLLA, poly(L-lactide), was mixed with PVA, poly(vinyl alcohol), at a ratio of 20:80 wt [Lin et al. (2014)]. The mixture was extruded at 180°C and the bristle was drawn at 75± 5°C. The PVA was then removed from this composite blend to create voids within the product by washing with and submerging in distilled water at 45± 5°C for 7-10 days. The remaining PLLA scaffold was cut into discs about 1.5cm across and about 1-3mm high. In order to prepare for cell culture, the scaffold was sterilized with 70% ethanol for 30 minutes. After residual ethanol was completely evaporated, the scaffold was washed with phosphate-buffered saline and immersed in cell culture medium at 37°C for 24 hours. The test for the biomaterial compatibility was performed twice. In each attempt, each scaffold was seeded with 0.4mL of mouse pre-osteoblastic cells (MC3T3-E1) at a concentration of 5x10⁴ cells/mL. On day 3, 7 10, 14, 20, the total cell population was estimated via AlamarBlue cell viability assays, which indicate the osteoblast population by the intensity of its fluorescence. Meanwhile, live/dead staining assays were performed to highlight the cell viability locally. Both the AlamarBlue intensity values and live/dead staining images were used to reconstruct the osteoblast concentration values for all of the days.

Computational: Our transductive machine learning approach can be summarized in six steps: 1) Using the finite element method to simulate the osteoblast cells growth;

³ Centre for Advanced Composite Materials, Department of Mechanical Engineering, the University of Auckland, Auckland 1010, New Zealand.

⁴ Department of Engineering Science, the University of Auckland, Auckland 1010, New Zealand.

2) Calculating root mean square errors between the simulation results and the experimental concentration; 3) Storing the errors and augmenting the training data set with the simulation results; 4) Retaining the support vector regression and predict the diffusivity values for cell-scaffold constructs; 5) Updating and storing the predicted diffusivity values; and6) repeat step 1 until convergence is reached. For step 1, we modelled cell migration with Fick's law of mass diffusion. The law is given as

$$J(x) = -D(\partial c / \partial x), \tag{1}$$

where diffusion flux, J, is proportional to the change in the spatial concentration of cell, c. The proportionality constant is the diffusivity, D. The minus sign infers that any highly concentrated cell clusters spread out. With the divergence theorem, we deduce the formation of Fick's second law which describes the temporal and spatial change of the solute concentration. Fick's second law is solved numerically by the finite element method in Abaqus using linear mass diffusion elements.

The support vector regression models are deployed to find the inverse of Fick's second law, thus deriving the diffusivity from the concentration values. It formulates a decision boundary as in equation (2) by minimizing objective function (3) so this primal function is rewritten as a dual optimization problem using Lagrange multipliers [Campbell and Ying (2011)]. It has been shown by applying the Karush-Kuhn-Tucker conditions, the solution lies on a saddle point. In equation (2), it is up to the user's discretion to ensure the chosen dot product suits the problem.

$$f(C) = w \bullet C + b, w \in X, b \in R \tag{2}$$

$$\min \frac{1}{2} \| w \|^2 \tag{3}$$

Results

The outcome from the transductive learning algorithm is an estimation of the diffusivity for each element in the PLLA scaffold. Figure 1 shows the iteration improvements on the estimation of the diffusivity values that lead to a better match between the simulation concentration values and the experimental concentration values. Specifically, concentration values from the experiment for PLLA are plotted on the top row, followed by the optimal simulation in the middle that provides the best match with the early initial guess at the bottom (improvements move from bottom to the top). The experiment shows the total living osteoblasts experience rise and falls in concentration over 3 weeks). It is reasonable to assume that the total osteoblast population is located on the surface because all scaffolds used were sliced thinly. It is worthy to note how the osteoblast concentration indeed varied both temporally and spatially, giving rise to an interesting pattern on how living osteoblasts migrate, proliferate, adhere on surfaces and grow. Osteoblasts appear to regroup: the highly concentrated neighborhood in earlier days no longer exists at the same spot in later days, and vice versa. Therefore, the concentration patterns are uneven not only spatially at each time point but also over the 3 week period.

The improvements in cell concentration estimation from increasing the number of iterations were obvious. As the number of iteration rises, the simulated concentration values show both global and local matches to those seen in the experiment. It is worthwhile to note how the mean of the concentration was first matched and later the spatial clusters of osteoblasts are partially captured. Our approach thus shows promising results as the support vector regression models morph themselves in order to refine the estimate of the diffusivity values that approach the concentration values from the experiment. In addition to visual examination on the similarity between the simulated concentration values from the transductive learning and the concentration values found in the experiment, we introduce the use of the Pearson product-moment correlation coefficients as a way to determine how the two are linearly associated. Their coefficients inform how linear proportionality between the simulated and the experimental. Between the PLLA, the coefficient is 0.0228 with a p-value of 0.312.

Thus, despite the similar appearance between the simulated and the experimental, we have seen evidence that the two are unlikely to be associated. It is well known that biological behaviours are highly non-linear and may explain why the coefficient is low.

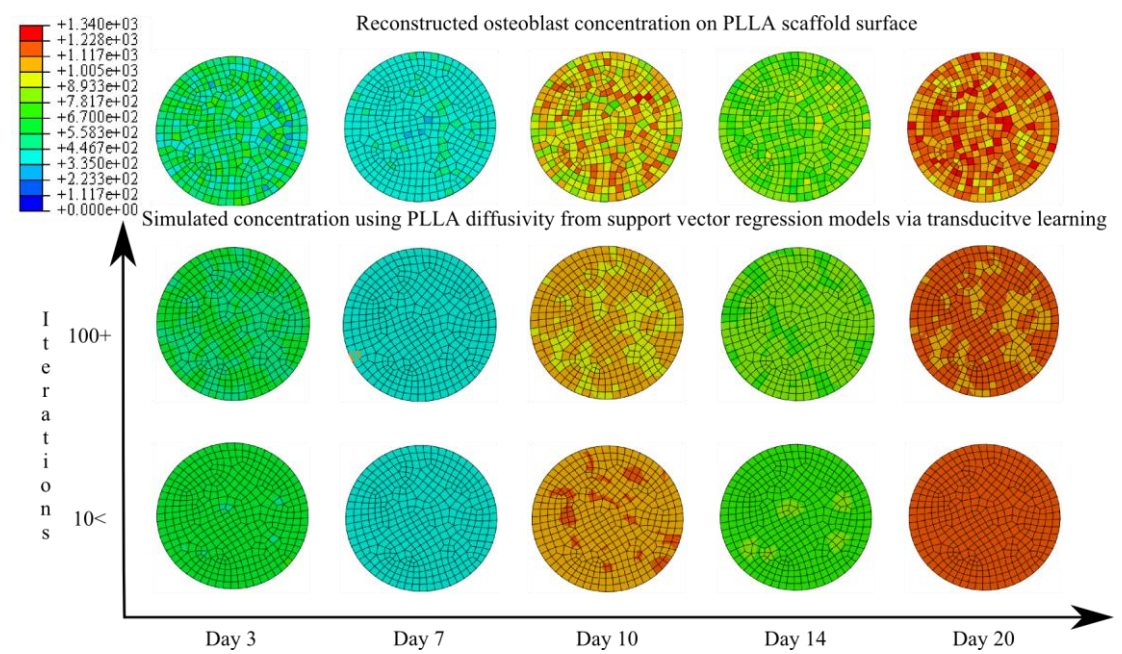


Figure 1 A summary of the transductive learning algorithm. The top row shows the raw experimental osteoblast concentrations over 3 weeks. The bottom two rows show the convergence of the solution after 100+ iterations. The optimal solution shows a consistent trend to the experimental data but differs in spatial regions.

Conclusions

The proposed transductive learning may be useful in estimating diffusivity in scaffolds from cell viability data. The transductive learning algorithm estimates the osteoblast diffusion given spatial and temporal data from an experiment. Its estimate is driven by and uniquely suited to the biological data. This is done without prior expert knowledge or manual input. Its diffusion prediction partly matches the observed on all days and thereby gives us some degree of confidence about the validity of the simulated diffusion on other unobserved days. This additional information may shed light on some biological and engineering questions. Nevertheless, our results should be interpreted with the following limitations in mind. By the nature of the algorithm, it does not guarantee a global optimum solution. Because of its slow convergence rate, it is even difficult to reach a local optimal. The poor convergence rate comes hand in hand with the resolving Fick's law and retraining the support vector regression models. The experimental data inform osteoblast behaviours on the specific days. However, the experiment data do not include further quantifiable information to accurately estimate the actual osteoblast concentration in the osteoblast-polymer construct. As part of the reconstruction of the osteoblast-polymer construct model, a possible improvement may be to weight "more recent" information as more salient and "less recent", less salient. Thus, a weighting scheme in the temporal dimension may be applied.

References

Colin, C. and Ying, Y. (2011). Learning with support vector machines. *Synthesis Lectures on Artificial Intelligence and Machine Learning* **5**(1),1–95.

Lin, S.T.C., Bhattacharyya, D., Fakirov, S., and Cornish, J. (2014). Novel Organic Solvent Free Micro-/Nano-fibrillar, Nanoporous Scaffolds for Tissue Engineering. *International Journal of Polymeric Materials and Polymeric Biomaterials* **63(8)**,416–423.